



Inclusion engineering of steel to prevent chemical tool wear

S. V. Subramanian^{*1}, H. O. Gekonde¹, G. Zhu¹, X. Zhang^{1,2}, U. Urlau³ and H. Roelofs³

¹ Department of Materials Science and Engineering, McMaster University, Hamilton, Ontario L8S 1C7, CANADA

² Currently with Technology Centre, Shanghai No.1 Iron & Steel Co., Baosteel, Shanghai 200126, CHINA

³ Research and Development Department, von Moos Stahl AG, 6021 Emmenbrücke, SWITZERLAND

* Corresponding author, e-mail subraman@mcmaster.ca

Iron and Steelmaking (2004) vol. 31 No3 p 249-257

Inclusion engineering of steel to prevent chemical tool wear

S. V. Subramanian*¹, H. O. Gekonde¹, G. Zhu¹, X. Zhang^{1,2}, U. Urlau³ and H. Roelofs³

Trent introduced the concept of tribological conditions of seizure at the tool–chip interface, when the normal pressure exceeds the flow stress of asperities so that the asperities are squeezed to make atomic contact. In consequence, chemical dissolution of the tool into the chip occurs by a diffusion mechanism, causing chemical wear. Oxley incorporated the concept of seizure in his quantitative model for flow chip morphology. Oxley introduced the concept of equilibrium shear angle in his quantitative model for flow chip morphology, which incorporates the work of shear in the secondary shear zone instead of friction, once atomic contact is established, but Oxley's model ignored potential interaction from metallurgical softening events in the secondary shear zone, which led to prediction of unrealistically high temperature at high cutting speeds. In fact, metallurgical softening events do occur particularly at high cutting speeds, causing shear localisation, which leads to significant deviation from Oxley's model predictions. In this paper, Oxley's model will be extended to capture the interaction of shear localisation in the secondary shear zone on the mechanics of metal cutting. Dynamic recrystallisation, phase transformation of the matrix and geometric softening owing to second phase particles are identified as important microstructural softening events causing shear localisation, which could intervene before the equilibrium shear angle is reached. The occurrence of shear localisation is shown to alter the mechanics of metal cutting, chip morphology and the tool wear mechanism. A phenomenological database in model alloys will be presented to validate the model assumptions. The application of the model in the design of self-lubricating free cutting steel for moderate and high cutting speeds will be examined.

Keywords: Metal cutting, Ferrous alloys, Chip formation, Softening, Tool wear

I&S/1856

Introduction

Merchant's model¹ on force diagram for metal cutting is based on a sliding tribological condition involving asperity contact at the tool–chip interface. Trent and his coworkers^{2,3} deduced from metallographic evidence that the tool–chip contact involved atomic contact at higher cutting speeds. Gekonde *et al.*⁴ proposed that tribological conditions of seizure occur at the tool–chip interface, when the normal stress exceeds the flow stress of the asperities. Under these conditions, the asperities are squeezed to make atomic contact. Once the atomic contact is established at the tool–chip interface, the work of shear in the secondary shear zone of the chip is

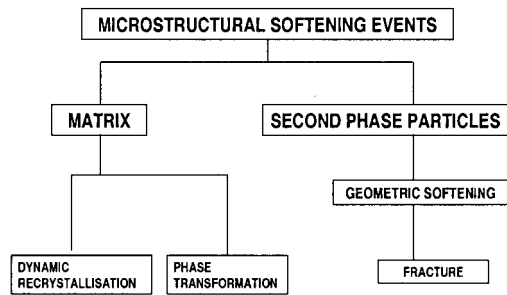
involved rather than friction in the sliding of asperities. Oxley incorporated this concept in his comprehensive model for flow chip morphology.⁵ Oxley's model for predicting equilibrium shear angle turns out to be the most comprehensive approach that incorporates both the mechanics of metal cutting and dynamic behaviour of metal during metal cutting. Oxley's prediction of equilibrium shear angle for flow chip morphology is validated in metal cutting at low cutting speeds. However, the domain of flow chip is limited by major microstructural softening events that occur at high cutting speeds particularly if the matrix is hardened by heat treatment or there is a large volume fraction of second phase particles. Dynamic recrystallisation and phase transformation are identified as major microstructural softening events occurring in the hardened matrix that cause shear localisation. Incompatibility of deformation between the matrix and second phase particles causes shear localisation because of geometric softening. Quantitative modelling to predict the critical speed for the onset of shear localised chip morphology

¹Department of Materials Science and Engineering, McMaster University, Hamilton, Ontario, Canada

²Currently with Technology Centre, Shanghai No.1 Iron & Steel Co., Baosteel, Shanghai, China

³Research and Development Department, von Moos Stahl, Emmenbrücke, Switzerland

*Corresponding author, e-mail subraman@mcmaster.ca



1 Microstructural softening events in metal cutting

requires quantitative database on the dynamic flow stress behaviour of materials that duly incorporates the microstructural softening events, which is the critical path. Quantitative analysis of the phenomenological database in model alloys has shown that shear localisation can be suppressed by engineering glassy oxide inclusions that lubricate *in situ* the tool–chip interface. This concept underlies the development of self-lubricating steel designed to suppress chemical wear in high speed machining.

Analysis

Basic science aspects of shear localisation in metal cutting

Metal cutting is a large strain, high strain rate deformation process in which the shear instability condition is attained in the primary shear zone. At large strains characteristic of the primary shear zone, shear instability occurs when the flow stress decrement caused by thermal softening overtakes the increment in flow stress caused by strain and strain rate hardening. Zener and Hollomon⁶ were the first to analyse the physics of large strain, high strain rate deformation behaviour of metals. They proposed that when the decrement in flow stress caused by thermal softening overtakes the increment in stress caused by strain hardening, plastic deformation becomes unstable and the homogeneous deformation gives way to a localised band-like deformation to form adiabatic shear bands. However, Meyers⁷ has pointed out that shear instability is a necessary but not an adequate condition for shear localisation. He has postulated that a major microstructural softening event is essential for shear localisation to occur. Meyers has demonstrated that dynamic recrystallisation is a major microstructural softening event that is effective in promoting shear localisation. Though most of the metal cutting is carried out under conditions of shear instability, shear localisation in chips is observed only under certain conditions, which are found to be dependent upon both material as well as metal cutting parameters. In the present work, it is shown that microstructural softening events cause shear localisation in metal cutting. Three competing microstructural softening events are identified that cause shear localisation in metal cutting (see Fig. 1). Dynamic recrystallisation and phase transformation are the two important microstructural softening events that occur in the matrix. Geometric softening is the third microstructural softening event that occurs owing to incompatibility of deformation between matrix and second phase particles, leading to plastic strain instability and fracture. The flow

localisation caused by the strain instability in the presence of voids is referred to as geometric softening. The large compressive stress occurring in the secondary shear zone at the tool–chip interface tends to suppress geometric softening in the secondary shear zone. However geometric softening is promoted by the state of stress in the primary shear zone, leading to fracture with or without the aid of shear localisation in the secondary shear zone. Therefore there are four possible cases of chip morphology arising from the shear localisation. The first case corresponds to flow chip morphology without shear localisation caused by any microstructural softening event. Merchant's model¹ applies to the first case with sliding tribology involving asperity contact at the tool–chip interface and Oxley's model⁵ applies to the same case but with the tribological conditions of seizure involving atomic contact at the tool–chip interface. The second case applies to shear localisation caused by microstructural softening in the primary shear zone but to the exclusion of shear localisation in the secondary shear zone. This second case has been investigated by Komanduri⁸ in alloys that are difficult to machine involving different crystal structure, i.e. Ti alloys with hcp structure, AISI 4340 steel in the hardened condition with bcc crystal structure, Inconel 720 with fcc crystal structure. The present work examines in depth the third case, where shear localisation occurs only in the secondary shear zone, and the fourth case, where shear localisation in the secondary shear zone is coupled to shear localisation in the primary shear zone.

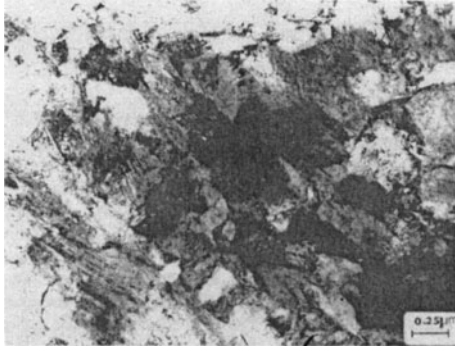
Most industrial cutting takes place under conditions of seizure involving atomic contact at the tool–chip interface, when microstructural softening events invariably occur in the secondary shear zone, causing shear localisation. Once shear localisation occurs in the secondary shear zone, the shear angle is decreased, which, in turn, causes shear localisation in the primary shear zone. The objectives of the present work are:

- (i) to gain a quantitative understanding of the role of microstructural softening events that cause shear localisation in the secondary shear zone
- (ii) to analyse how the shear localisation in the secondary shear zone influences shear localisation in the primary shear zone in a coupled manner
- (iii) to identify methods to suppress chemical tool wear caused by shear localisation.

Physics of shear localisation caused by microstructural softening events

Detailed metallographic characterisation of chips generated at higher cutting speeds in a range of model iron alloys with and without second phase particles both in the hardened and unhardened condition by heat treatment showed evidence of microstructural softening events caused by phase transformation and dynamic recrystallisation. The weakening of mechanical properties of a polycrystal while it is undergoing phase transformation causes shear localisation in the case of phase transformation.⁹

These microstructural softening events ought to occur within exceedingly short deformation time, which is typically 10^{-4} – 10^{-5} s. Meyers¹⁰ has clarified that sub-grain rotation is the underpinning mechanism of

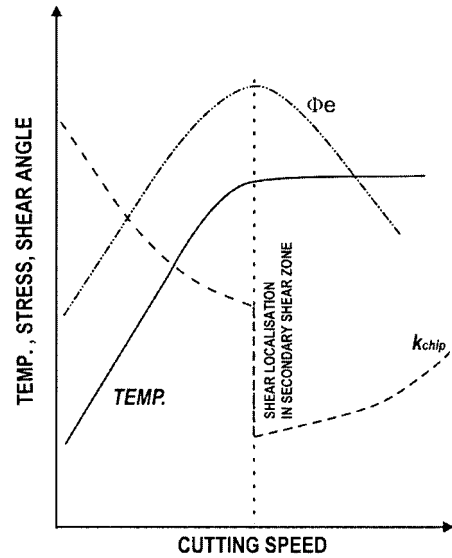


2 TEM picture of secondary shear zone in the chip generated during machining an AISI/SAE 1045 steel with a cemented tungsten carbide (K-11) tool at a cutting speed of 240 m min^{-1} . Note the ultrafine grains with a diameter of about $0.25 \mu\text{m}$

dynamic recrystallisation causing shear localisation during large strain, high strain rate deformation. The typical recrystallised grain size obtained by the rotation mechanism is very small in the range of $0.1\text{--}0.3 \mu\text{m}$, which is comparable to what is observed in the secondary shear zone in metal cutting. According to this model, the typical temperature at which the rotational mechanism of dynamic recrystallisation operates is, T_m being the melting point temperature, about $(0.45\text{--}0.5)T_m$, which, in the case of steel is $550\text{--}630^\circ\text{C}$. Because the phase transformation temperature is higher than the temperature of dynamic recrystallisation in steel, it is surmised that the dynamic recrystallisation will precede phase transformation to cause shear localisation in the secondary shear zone in the case of steel chips. Figure 2 shows a TEM picture of the secondary shear zone in the chip from machining of AISI/SAE 1045 steel using a cemented tungsten carbide tool (K-11) at a cutting speed of 240 m min^{-1} , exhibiting ultra-fine grains of about $0.25 \mu\text{m}$. Electron diffraction studies confirmed the presence of twinned martensitic structure and this serves as evidence for austenitisation of steel in the secondary shear zone. Whether shear localisation was initiated by dynamic recrystallisation followed by phase transformation to austenite or vice versa remained an issue that warranted further investigation using Fe–Ni–C model alloys with varying phase transformation temperatures.

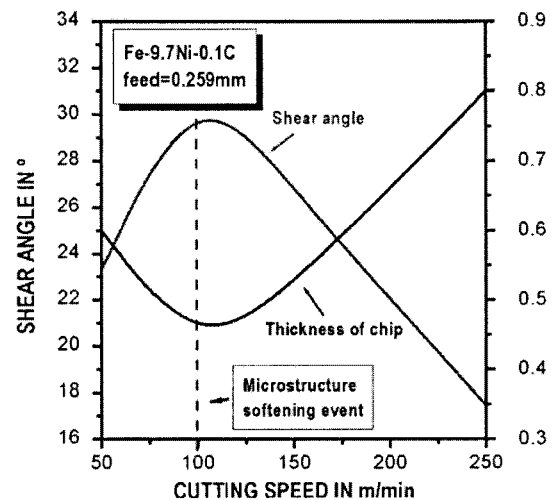
Effect of shear localisation on Oxley's model

Oxley's model⁵ does not consider shear localisation in the secondary shear zone and for this condition the model predicts that the flow stress in the secondary shear zone will decrease with the increase in cutting speed. The flow stress decrement caused by temperature rise (the thermal softening effect) dominates over the flow stress increment because of strain rate increase from higher cutting speed (strain rate hardening effect). Oxley⁵ therefore predicted that the shear angle would increase with cutting speed, but once shear localisation occurs in the secondary shear zone, the reverse is true, i.e. the strain rate hardening effect dominates over the thermal softening effect, causing a net increase in the flow stress in the secondary shear zone with increase in cutting speed. In consequence, shear angle will decrease with cutting speed.

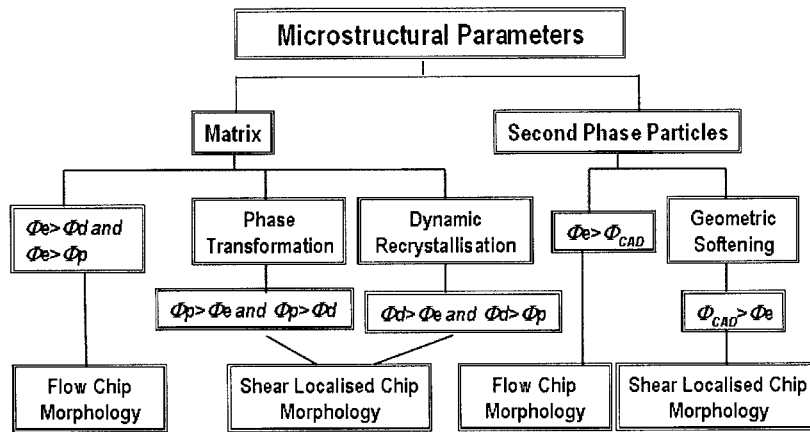


3 Schematic showing the effect of shear localisation in the secondary shear zone on the variation in temperature, shear flow stress in the secondary shear zone k_{chip} and equilibrium shear angle Φ_e with cutting speed

There are two important factors, which could account for the increase in flow stress in the secondary shear zone with cutting speed upon shear localisation. The first one is the strain rate sensitivity of the material that increases the flow stress owing to the dislocation drag mechanism.⁷ The second effect is due to the temperature saturation effect caused by flow stress decrease accompanying microstructural softening event.⁴ Therefore it is concluded that upon shear localisation in the secondary shear zone, the temperature saturation effect coupled with the strain rate hardening effect by dislocation drag mechanism will increase the flow stress in the secondary shear zone with cutting speed. This, in turn, will cause the shear angle to decrease with increase in cutting speed (see Fig. 3). This is consistent with metallographic results on chip morphology, which shows an increase in chip thickness with cutting speed in hardened Fe–Ni–C model alloys (see Fig. 4). Model Fe–Ni–C alloys are heat



4 The variation of measured thickness of flow chip and the calculated shear angle with cutting speed obtained in cutting hardened Fe–9.7Ni–0.1C alloy at a constant feed of 0.259 mm and a positive rake angle of $+5^\circ$



5 Onset of shear localised chip morphology as a function of cutting parameters. The onset of the shear localised chip morphology occurs when the critical shear angle Φd or Φp or Φ_{CAD} exceeds the equilibrium shear angle Φe . (Φe is the equilibrium shear angle, Φp is the critical shear angle for phase transformation, Φd is the critical shear angle for dynamic recrystallisation and Φ_{CAD} is the critical shear angle for critical accumulated damage)

treated to martensitic structure. These alloys are designed to exhibit microstructural softening because of reverse martensite to austenite phase transformation in the short deformation time characteristic of metal cutting. In the model alloys the reverse martensite to austenite phase transformation temperature is varied independently through varying nickel content of the alloy. Further, the work hardened martensite is known to soften by recrystallisation.

The most important consequence of the decrease of the shear angle with the increase in cutting speed owing to shear localisation in the secondary shear zone is to promote shear localisation in the primary shear zone. Any one of the three competing microstructural softening events could cause shear localisation in the primary shear zone. With the decrease in shear angle, it is possible that the strain in the primary shear zone is increased beyond the critical strain for dynamic recrystallisation or the temperature is raised to attain the phase transformation. The flow stress decrease accompanying either of the microstructural softening events in the primary shear zone causes the occurrence of shear localisation in the primary shear zone. Alternatively the strain in the primary shear zone could exceed the critical strain for fracture in the case of materials with low critical accumulated damage to fracture, causing segmentation in the primary shear zone.

The critical strain for dynamic recrystallisation is a function of Z , the Zener–Hollomon parameter in the primary shear zone.¹¹ The critical speed for the onset of shear localisation by dynamic recrystallisation is predicted when the shear strain in the primary shear zone exceeds the critical strain for dynamic recrystallisation and the corresponding shear angle Φd is defined as the critical shear angle for dynamic recrystallisation. By the same token, shear localisation caused by phase transformation is predicted when the temperature on the primary shear plane exceeds the phase transformation temperature. The corresponding critical shear angle is defined as Φp . In the case of geometric softening the fracture criterion is based on the concept of critical accumulated damage. This material parameter is independent of the state of stress. The critical accumulated damage to fracture is a material property that is

decreased by an increase in volume fraction of second phase particles and hardening of the matrix.¹² The incompatibility of deformation between the particle and the matrix causes damage to occur. The damage mechanism involves void nucleation, which is influenced by second phase particle size, dispersion, and interfacial bonding strength between the particle and the matrix. The void growth rate is governed by matrix plasticity. With the increase in cutting speed, the damage (void growth) rate is increased because the increase in flow stress owing to strain rate hardening of the matrix decreases the ratio of hydrostatic pressure over flow stress (P/k ratio), making it more tensile. The effect of decreasing the feed is to increase hydrostatic pressure, which decreases damage rate. A quantitative model¹³ has been developed that is based on continuous nucleation of voids with plastic strain coupled with McClintock's void growth model to quantify damage accumulation in the primary shear zone. When the critical strain for fracture is exceeded, segmentation of the chip owing to geometric softening is predicted, the critical shear angle is defined as Φ_{CAD} . Therefore physically based models are available for the prediction of the onset of shear localisation in the primary shear zone as a function of cutting speed by any one of the three microstructural softening events as shown in Fig. 5. The onset of the shear localised chip morphology occurs when the critical shear angle Φd or Φp or Φ_{CAD} exceeds the equilibrium shear angle Φe such that shear localisation event intervenes before the steady state equilibrium shear angle for flow chip morphology is reached. The results of quantitative analysis are in agreement with the available experimental database in general. However, the lack of a reliable database to describe the dynamic flow stress behaviour of material at the large strains and high strain rates characteristic of metal cutting in experimental model alloys has turned out to be the critical path in validating the quantitative model predictions rigorously.

Consequence of shear localisation

Shear localisation in the secondary shear zone caused by dynamic recrystallisation or phase transformation provides high diffusivity paths through ultra-fine grains,

which accelerate the chemical dissolution of the tool into the chip by diffusion mechanism. This causes crater wear to occur on the rake face of the tool at the tool–chip interface, but a more important effect of shear localisation in the secondary shear zone is to promote shear localisation in the primary shear zone in a coupled manner. Once shear localisation occurs in the primary shear zone owing to dynamic recrystallisation or phase transformation, enhanced diffusional wear is localised at the cutting edge of the tool, where the primary shear zone contacts the tool. Figure 6a shows shear localised chip morphology caused by the reverse martensite to austenite phase transformation occurring at 400°C in machining Fe–28.9Ni–0.1C alloy at a cutting speed of 456 m min⁻¹ and Fig. 6b shows the consequent chemical wear localised at the cutting edge of the tool. Figure 6c is a dark field image from TEM diffraction of the shear localised region in the primary shear zone shown in Fig. 6a, exhibiting ultra-fine dynamically recrystallised grains of about 20 nm dia.

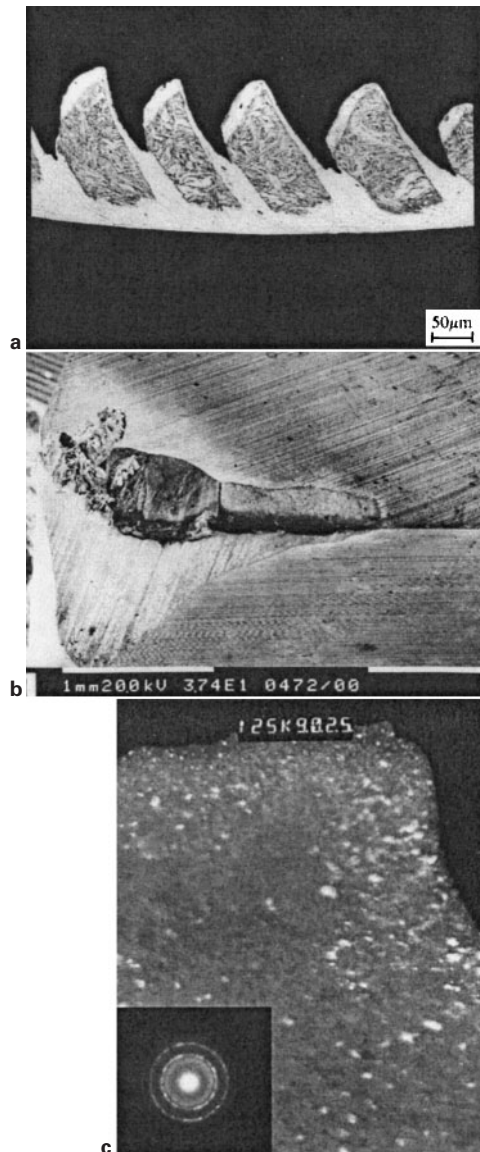
Mechanism of accelerated chemical tool wear

Ingle¹⁴ quantified chemical wear by measuring atomically dissolved tungsten in the chips generated during machining AISI 1045 steel with cemented tungsten carbide tool as a function of cutting speed. Quantitative analysis of diffusional wear showed that high diffusivity paths are required in order to reconcile the experimental results with theoretical prediction. Grain boundary diffusion of the nanocrystalline grains formed in the interfacial layer at the tool–chip interface is identified as the dominant mechanism that causes accelerated chemical wear.

The effect of microstructural softening caused by dynamic recrystallisation is expected to occur at a temperature around 0.45–0.5 T_m . Normally, in metal cutting, the strain rate is in the order of 10⁴–10⁶. In this case the Zener–Hollomon parameter is in the order of 10²²–10²⁴, with the corresponding dynamically recrystallised grain size ranging from 40 to 12 nm. The nanocrystalline grain boundary provides the high diffusivity path, causing accelerated chemical wear. Quantitative modelling of chemical diffusional wear in nanocrystalline grains shows that the accelerated diffusion is caused by

- (i) the increased grain boundary volume of nanocrystalline grains (20–30 vol.-%)
- (ii) high solubility of solute in the nanocrystalline grain boundary (two to three orders of magnitude in the grain boundary more than that inside the grain in some cases)
- (iii) high diffusivity in the nanocrystalline grain boundary, which is eight to ten orders magnitude greater than in the lattice (typically one to three orders of magnitude greater than that in the polycrystalline grain boundary).

Therefore the mechanism of accelerated chemical tool wear is caused by high diffusivity in the nanocrystalline grain boundary. The occurrence of nanocrystalline grains is, in turn, caused by shear localisation because of microstructural softening by dynamic recrystallisation under a large Z condition.



6 a Optical microstructure of the chip obtained at a cutting speed of 456 m min⁻¹ in Fe–28.9Ni–0.1C alloy hardened by heat treatment. Shear localisation in the primary shear zone of the chip is caused by the reverse martensite to austenite phase transformation. TEM examination of the transformation shear band in the primary shear zone showed ultra-fine grains of <0.1 μm, which are attributed to dynamic recrystallisation. b Interaction of the primary shear zone at high temperature with the cutting edge of the tool raises the temperature at the cutting edge. Oxidation and dissolution chemical wear are localised at the cutting edge, resulting in loss of the cutting edge of tool. c Dark field image from TEM diffraction of shear localised region in the primary shear zone shown in Fig. 5a, exhibiting ultra-fine recrystallised grains of about 20 nm dia. Each bright region is an individual crystallite

Synthesis

Strategies to prevent chemical wear

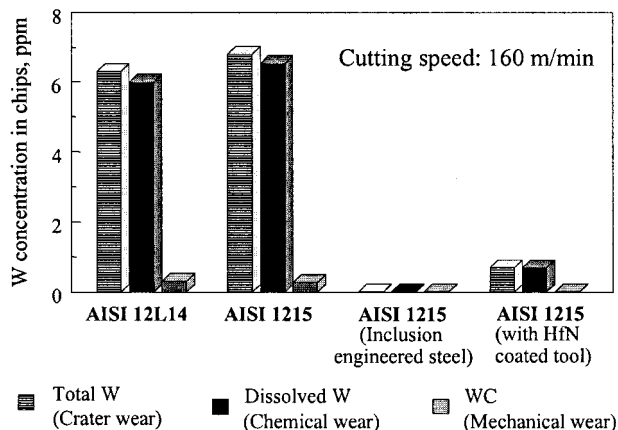
Because chemical wear is caused by high diffusivity paths owing to nanocrystalline grains associated with

shear localisation, the best strategy to prevent chemical wear is to suppress shear localisation. Because the tribological conditions of seizure at the tool–chip interface cause shear localisation in the secondary shear zone, it is possible to suppress shear localisation in the secondary shear zone by lubricating the tool–chip interface. The effect of *in situ* lubrication at the tool–chip interface using glassy oxide inclusions dispersed in the workpiece is to minimise the energy expended in the secondary shear zone. The smaller the energy consumed in the secondary shear zone, the larger the equilibrium shear angle. In consequence, the strain and the temperature in the shear plane will be low, which, in turn, will suppress shear localisation in the primary shear zone. In consequence, chemical wear at the cutting edge of the tool can be prevented.

Engineering of oxide inclusions for enhanced tool life

‘In the macroscopic case of liquid lubrication, the shearing is taking place within the bulk liquid (that is at a liquid–liquid interface) which usually offers less resistance to shearing (friction) than does a solid–liquid interface.’¹⁵ This principle underlies the concept of inclusion engineering of steels for *in situ* lubrication of the tool–chip interface. The steel is designed to be self-lubricating by modifying the rheology of existing oxide inclusions normally present in steel after deoxidation. Glassy inclusions are designed to soften at the tool–chip interface temperature and form *in situ* a viscous layer of adequate thickness so that the shear is accommodated within the viscous layer.¹⁶ Therefore, the viscous layer of glass (super-cooled liquid) formed *in situ* lubricates the tool–chip interface, thereby preventing the occurrence of tribological phenomenon of seizure. The base chemistry of the melt and deoxidation process are controlled so that both exogenous (formed directly in the melt by deoxidation) and indigenous inclusions (formed during solidification of the melt) are glassy in inclusion engineered steel.¹⁷ It should be emphasised that the volume fraction of inclusions required to lubricate the tool–chip interface is very small, being of the order of about 10^{-4} . The technological implication is that inclusion engineering is merely modification of existing oxide inclusions in steel. The process of inclusion engineering requires clean steel practice. The efficacy of the viscous layer in suppressing the tribological phenomenon of seizure was investigated in free cutting steels. Glassy oxide inclusions engineered into AISI 1215 were demonstrated to be more effective than the HfN coating in suppressing dissolution crater wear (see Fig. 7).¹⁸

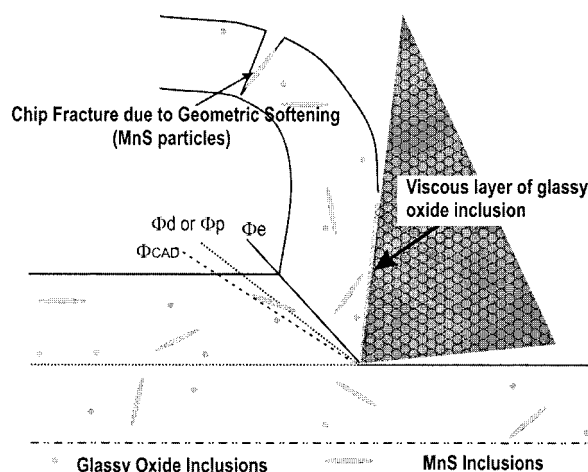
Ingle carried out secondary ion mass spectrometry (SIMS) analysis of W and Co in the chip generated from machining 1045 steel from 150 to 240 $m\ min^{-1}$. The depth profile of W and Co into the chip exhibited features characteristic of the diffusion profile. The depth of penetration of tungsten was found to increase with cutting speed, confirming that the mechanism is controlled by the thermally activated diffusion process. The depth of W penetration at 240 $m\ min^{-1}$ was typically 500 nm. The amount of tungsten that is atomically dissolved into the chip is quantified using instrumental neutron activation analysis by a method originally developed by Ingle¹⁹ and this is used as a



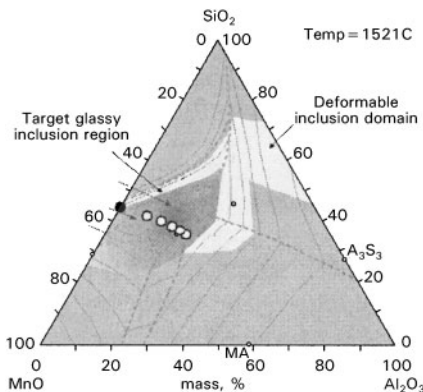
7 Comparison of tool wear in machining of leaded (AISI 12L14), non-leaded AISI 1215 and inclusion engineered AISI 1215 free cutting steels with uncoated cemented carbide (K1) tool and with HfN coated cemented carbide tool (AISI 1215) at a cutting speed of $160\ m\ min^{-1}$

quantitative measure of chemical wear. All the chips generated at a given cutting speed for a given time were collected and irradiated in a neutron flux of 10^{12} neutron $cm^{-2}\ s^{-1}$. The total amount of tungsten present in the chips was determined using standards of known composition; the total is made up of tungsten atomically dissolved in the iron matrix plus tungsten present as tungsten carbide particles. The chips were then dissolved in concentrated hydrochloric acid and the tungsten present as tungsten carbide retained in the undissolved residue was determined. The tungsten in solution was taken as the difference, i.e. the total tungsten in the chips less the tungsten tied up as tungsten carbide. Inductively coupled plasma-mass spectrometric (ICP-MS) analysis can be used to determine the minute concentration of tungsten in the chip instead of neutron activation analysis.^{20,21}

By preventing the tribological phenomenon of seizure through inclusion engineering, it is demonstrated that it is possible to prevent chemical wear of the tool by suppressing shear localisation in the secondary and



8 Schematic illustration of optimal microstructural design for the control of chip morphology, chip disposal and minimal tool wear. The condition for flow chip morphology occurs because $\Phi_e > \Phi_d$ or Φ_p or Φ_{CAD}



9 Indigenous glassy oxide inclusions reaction path as controlled by melt chemistry following slag-metal equilibration (model prediction)

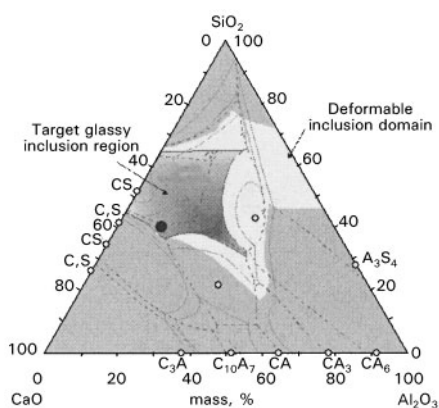
therefore primary shear zones. In the design of free cutting steel, it is important to control the rheology of oxide inclusions in order to suppress shear localisation at the tool-chip interface. The glassy oxide inclusions are designed to lubricate the tool-chip interface *in situ*, thereby preventing the occurrence of shear localisation in the secondary shear zone and therefore shear localisation in the primary shear zone. In consequence steady state flow chip morphology is obtained, which is the target.

Engineering of sulphide inclusions for ease of chip fracture

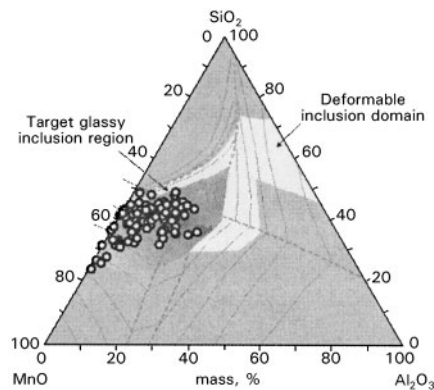
In the case of flow chip morphology, chip disposal could pose a problem. Geometric softening owing to second phase particles on a microstructural scale will facilitate chip segmentation. Adequate volume fraction of MnS inclusions is ensured by resulfurisation in order to lower the critical accumulated damage so that the chip fractures at the chip breaker for the working range of cutting parameters. The schematic in Fig. 8 illustrates the features of optimal microstructural design for the control of chip morphology, chip disposal and minimal tool wear.

Industrial application

Through process modelling capability based on the concept of product-process integration has been



11 Exogenous inclusions are modified by Ca treatment to obtain glassy inclusions (model prediction)



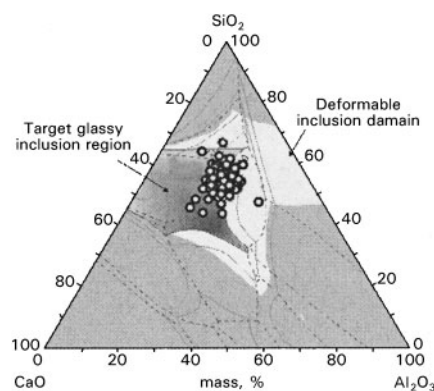
10 EDS analysis of indigenous oxide inclusions of MnO-Al₂O₃-SiO₂ in 11SMn37 IE steel as rolled (experimental validation of model prediction)

developed to produce inclusion engineered steels with enhanced machinability. The product requirement is glassy oxide inclusions, which lubricate the tool-chip interface. Thermodynamic modelling of slag-metal equilibration is used for deoxidation control to produce the target glassy oxide inclusions. The following case study of non-leded inclusion engineered steel produced under industrial conditions at von Moos Stahl and laboratory machinability evaluation of the inclusion engineered steel carried out independently at three laboratories demonstrates the importance of inclusion engineering in controlling the flow chip morphology and in minimising chemical tool wear.

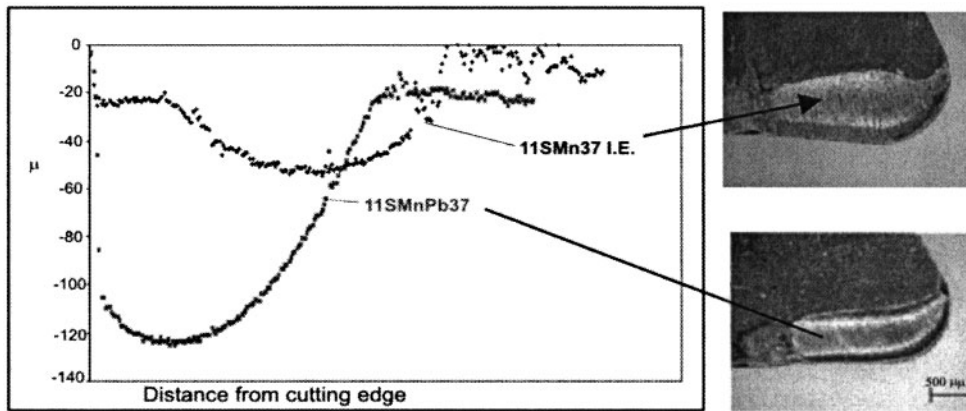
Production of inclusion engineered non-leded free cutting steels

At von Moos Stahl, four 70 ton heats of the inclusion engineered non-leded steel grade 11SMn37 IE ('inclusion engineered') were cast, rolled and drawn to 30 and 35 mm bright bars. Through process modelling capability was developed for deoxidation control of the melt from primary deoxidation through to the caster. The modelling was used for online process control of slag chemistry.

The thermodynamic model for inclusion engineering is based on slag-metal equilibration. The model predictions of indigenous and exogenous inclusion compositions are given in Figs. 9 and 11 respectively. The actual compositions measured on a number of indigenous and exogenous inclusions in the bars are mapped on the



12 EDS analysis of exogenous oxide inclusions of CaO-Al₂O₃-SiO₂ (A) 11SMn37 IE steel as rolled (model validation)



13 Optical line scans through the crater of two HM tools after machining of 11SMn37 IE or 11SMnPb37 respectively. The pictures of the tools are shown. Cutting parameters were: cutting speed=300 m min⁻¹, cut depth=2 mm, feed rate=0.3 mm U⁻¹, tool travel=4112 m, dry machining

relevant ternary diagrams shown in Figs. 10 and 12 respectively. The close agreement between the predicted and measured inclusion compositions serves to validate the model.

Machinability evaluation of inclusion engineered non-lead free cutting steels

The machinability characterisation of IE steel in comparison to the standard steel grade 11SMnPb37 was carried out independently at three different laboratories, namely IFW, University of Hannover, the IWF, ETHZ, Zürich and MMRI, McMaster University, Hamilton, Canada. Some salient results are shown in the following sections.

Crater wear

To determine crater wear, machining tests at 300 m min⁻¹ were performed with HM tools without chip breaking geometry. The crater wear was measured optically by performing line scans (Fig. 13). The effect of inclusion engineering is to lubricate *in situ* the tool-chip interface, which reduces the crater wear.

Flank wear

Tool life is measured by using a flank wear criterion. The tool life criterion was the time to reach 0.3 mm flank wear. Four heats of steel grade 11SMnPb37 (two suppliers) and four heats of 11SMn37 IE were tested. A comparison of flank wear results shows that the non-lead inclusion engineered grade gives a better tool life than the leaded grade particularly at higher cutting speed. See Fig. 14a and b.

Results

- (i) Non-lead oxide inclusion engineered steel is shown to enhance tool life compared to leaded steel at cutting speeds above 100 m min⁻¹.
- (ii) The improvement in tool life is attributed to sliding tribology promoted by *in situ* lubrication of glassy oxide inclusions at the tool-chip interface.
- (iii) Besides reduced tool wear and improved surface finish, the sliding tribology by inclusion engineering offers the distinct advantage of control of flow chip morphology.

- (iv) In the absence of *in situ* lubrication at the tool-chip interface, adhesion between the tool and the chip would occur. The intense deformation in the chip triggers microstructural softening, which causes shear localisation to occur. High diffusivity paths associated with shear localisation accelerate chemical wear of the tool into the chip by diffusion mechanism. Shear localisation and therefore accelerated chemical tool wear can be prevented by *in situ* lubrication of the tool-chip interface through inclusion engineered steel.

Conclusions

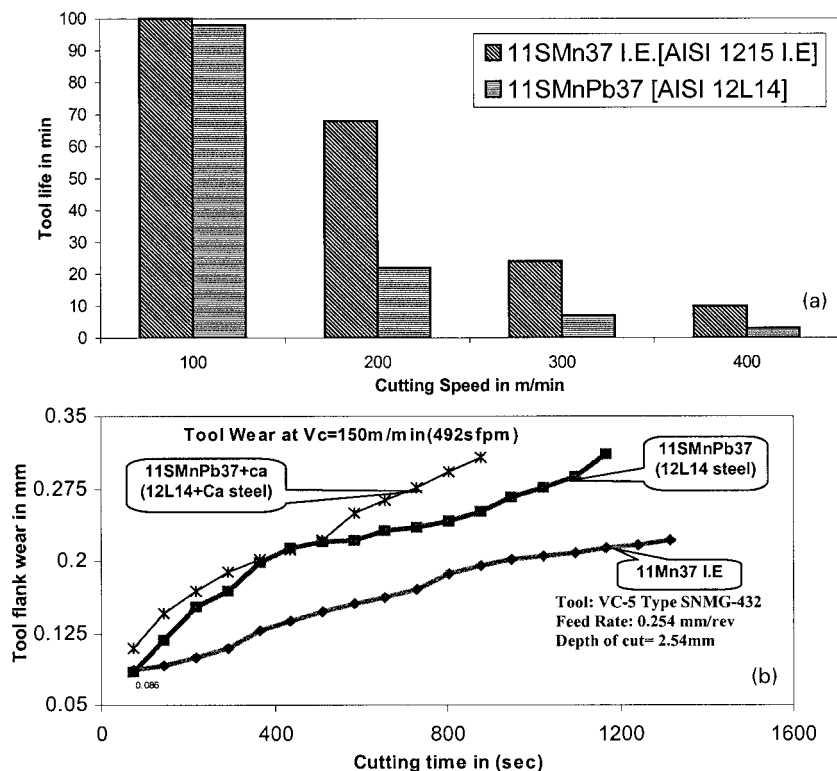
The dynamic behaviour of workpiece material is not necessarily well behaved with temperature, strain rate and strain as captured in constitutive equations because the microstructural softening events can occur abruptly at critical values of these parameters, causing shear localisation to occur. Phase transformation, dynamic recrystallisation and fracture are the three microstructural softening events that occur at critical values of temperature, strain rate and strain respectively.

Once microstructural softening events cause shear localisation in the secondary shear zone, the shear angle decreases with cutting speed, thereby promoting the onset of shear localisation in the primary shear zone.

If the intervention of microstructural softening event were to occur before the equilibrium shear angle for flow chip morphology is reached, the onset of shear localised chip morphology is predicted. Oxley's model for flow chip morphology is extended to predict the onset of shear localised chip morphology.

Shear localisation provides high diffusivity paths through nanocrystalline grain boundary, which accelerate chemical diffusional wear. The high solubility of tool material in the nanocrystalline grain boundary, high volume fraction of the nanocrystalline grain boundary and the high diffusivity in the nanocrystalline grain boundary are the three contributing factors for the accelerated diffusion of tool material into the chip.

Lubricating *in situ* with glassy oxide inclusions engineered into the steel workpiece can prevent the accelerated chemical wear from dynamically recrystallised nanocrystalline grains.



14 a Tool life to reach a flank wear of 0.3 mm; feed rate, 0.1 mm rev^{-1} , depth of cut, 1 mm, dry machining condition, uncoated HM tool. b Tool flank wear rate at a cutting speed of 150 m min^{-1} at a feed rate of $0.254 \text{ mm rev}^{-1}$ (tool VC-5, SNMG-432)

The concept of inclusion engineering to minimise chemical wear by lubricating the tool-chip interface with a viscous layer of glassy oxide inclusions formed *in situ* is validated by machining results obtained from inclusion engineered industrial heats of non-lead free cutting steel of AISI 1215 and 11SMn37 IE.

Acknowledgements

We dedicate this paper to the memory of Professor R. Sowerby, who provided the inspiration and research support for this work. We wish to acknowledge with grateful thanks research support from NSERC, Canada and Materials and Manufacturing of Ontario (MMO). We acknowledge with thanks helpful discussion with Dr M. ElBestawi, Dr J. D. Embury, Dr G. C. Weatherly and Dr G. R. Purdy of McMaster University and Dr C. M. Sellars of Sheffield University, UK. We thank Mr S. Lemgen, Mr W. Fuchs and Dr M. Kuhnemund of von Moos Stahl for help in production trials of IE steel. We thank S. Patil and Dr S. Veldhuis of McMaster University for machinability evaluation of inclusion engineered steel. Updated from a presentation at the 5th Int. Conf. on 'Behaviour of materials in machining' organised by the Steel Division of IOM³ in Chester, UK on 12–13 November 2003.

References

1. M. E. Merchant: *J. Appl. Mech.*, 1944, **A11**, 168–175.
2. E. M. Trent: *Metal Cutting*, 3rd edn; 1991, Oxford, Butterworth-Heinemann.

3. E. M. Trent: *Wear*, 1988, **128**, 47–64.
4. H. O. Gekonde and S. V. Subramanian: in Proc. 1st French and German Conf. on 'High speed machining', (ed. A. Molinari *et al.*), 1997, University of Metz, 49–62.
5. P. L. B. Oxley: *Mach. Sci. Technol.*, 1998, **2**, 65–189.
6. C. Zener and J. H. Hollomon: *J. Appl. Phys.*, 1944, **15**, 22–32.
7. M. A. Meyer: *Dynamic Behaviour of Materials*; 1995, New York, Wiley.
8. R. Komanduri: *Wear*, 1982, **76**, 15–34.
9. G. W. Greenwood and R. H. Johnson: *Proc. R. Soc. (London)*, 1965, **A183**, 403–422.
10. M. A. Meyers, V. F. Nesterenko, J. C. LaSavia and Q. Xue: *Mat. Sci. Eng. A*, 2001, **A317**, 204–225.
11. G. Zhu, D. Tan and S. V. Subramanian: *ISS Mech. Work. Steel Process. Conf. Proc.*, 2000, **38**, 757–768.
12. R. Sowerby and N. Chandrasekaran, *Mater. Sci. Eng.*, 1986, **79**, 27–36.
13. S. V. Subramanian, D. A. R. Kay, N. Chandrasekaran and R. Sowerby: in Proc. ASM Int. Conf. on 'Strategies for automation of machining: materials and processes', 27–42; 1987.
14. S. S. Ingle: 'The mechanisms of cemented carbide cutting tool wear', PhD thesis, McMaster University, Hamilton, ON, Canada, 1993.
15. J. Krim: *Scient. Am.*, 1996, **275**, 74–80.
16. S. V. Subramanian and D. A. R. Kay: *ISS Mech. Work. Steel Process. Conf. Proc.*, 1997, **34**, 125–135.
17. S. V. Subramanian, H. O. Gekonde, X. Zhang and J. Gao: *Ironmaking Steelmaking*, 1999, **26**, 333–338.
18. K. Ramanujachar and S. V. Subramanian: *Wear*, 1996, **197**, 45–55.
19. S. V. Subramanian, S. S. Ingle and D. A. R. Kay: *Surf. Coat. Technol.*, 1993, **61**, 293–299.
20. H. O. Gekonde and S. V. Subramanian: *Surf. Coat. Technol.*, 2002, **149**, 151–160.
21. H. O. Gekonde: 'Influence of dynamic behaviour of materials on machinability', PhD thesis, McMaster University, Hamilton, ON, Canada, 1998.